




Article

System Profit Improvement of a Thermal–Wind–CAES Hybrid System Considering Imbalance Cost in the Electricity Market

Mitul Ranjan Chakraborty¹, Subhojit Dawn^{2,*} , Pradip Kumar Saha³, Jayanta Bhusan Basu¹ 
and Taha Selim Ustun^{4,*} 

¹ Department of Electrical Engineering, Siliguri Institute of Technology, Darjeeling 734009, West Bengal, India

² Department of Electrical & Electronics Engineering, Velagapudi Ramakrishna Siddhartha Engineering College, Vijayawada 520007, Andhra Pradesh, India

³ Department of Electrical Engineering, Jalpaiguri Government Engineering College, Jalpaiguri 735102, West Bengal, India

⁴ Fukushima Renewable Energy Institute, AIST (FREA), Koriyama 963-0298, Japan

* Correspondence: subhojit.dawn@gmail.com (S.D.); selim.ustun@aist.go.jp (T.S.U.)

Abstract: Studying a renewable energy integrated power system's features is essential, especially for deregulated systems. The unpredictability of renewable sources is the main barrier to integrating renewable energy-producing units with the current electrical grid. Due to its unpredictable nature, integrating wind power into an existing power system requires significant consideration. In a deregulated electricity market, this paper examines the implications of wind farm (WF) integration with CAES on electric losses, voltage profile, generation costs, and system economics. Comparative research was done to determine the impact of wind farm integration on regulated and deregulated environments. Four randomly chosen locations in India were chosen for this investigation, together with real-time information on each location's real wind speed (RWS) and predicted wind speed (PWS). Surplus charge rates and deficit charge rates were created to assess the imbalance cost arising from the discrepancy between predicted and real wind speeds to calculate the system economics. When the effect of imbalance cost is considered, the daily system profit shows a variation of about 1.9% for the locations under study. Customers are always seeking electricity that is dependable, affordable, and efficient due to the reorganization of the power system. As a result, the system security limit could be exceeded or the system might function dangerously. The final section of this paper presents an economic risk analysis using heuristic algorithms such as sequential quadratic programming (SQP), artificial bee colony algorithms (ABC), and moth flame optimization algorithms (MFO). It also discusses how the CAES is used to correct the deviation of WF integration in the real-time electricity market. Economic risk analysis tools include value-at-risk (VaR) and conditional value-at-risk (CVaR). The entire piece of work was validated using a modified IEEE 30-bus test system. This work shows that with a three-fold increase in wind generation, the risk coefficient values improves by 1%.

Keywords: regulated system; deregulated system; wind energy; compressed air energy storage; system profit; value-at-risk; conditional value-at-risk



Citation: Chakraborty, M.R.; Dawn, S.; Saha, P.K.; Basu, J.B.; Ustun, T.S. System Profit Improvement of a Thermal–Wind–CAES Hybrid System Considering Imbalance Cost in the Electricity Market. *Energies* **2022**, *15*, 9457. <https://doi.org/10.3390/en15249457>

Academic Editor: Surender Reddy Salkuti

Received: 21 October 2022

Accepted: 8 December 2022

Published: 13 December 2022

Publisher's Note: MDPI stays neutral with regard to jurisdictional claims in published maps and institutional affiliations.



Copyright: © 2022 by the authors. Licensee MDPI, Basel, Switzerland. This article is an open access article distributed under the terms and conditions of the Creative Commons Attribution (CC BY) license (<https://creativecommons.org/licenses/by/4.0/>).

1. Introduction

In a deregulated electricity market, profit maximization using energy storage systems is determined by the price of electricity. In the past, electricity markets were not allowed to be deregulated, as they were considered a 'natural monopoly' [1]. However, lately, there has been a shift toward deregulation of the electricity market. This has resulted in increased competition between market players, i.e., generation companies (GENCOs), transmission companies (TRANSCOs), distribution companies (DISCOs), and customers, which has led to lower prices for consumers [2]. Energy storage systems can help power providers to maximize profits by ensuring that they will have sufficient energy at all times. Energy storage systems allow power companies to store electricity and use it when it is needed [3].

To meet the rising global power claims in this climate, renewable energy must be used alongside existing non-renewable energy sources. Wind energy has risen to first place in recent decades as the world's most rapidly expanding source of electrical energy, with rapid annual expansion over the period. Wind power (being carbon-free) generation minimizes carbon output to a large extent, which is an important aspect of the transition away from fossil fuels. Many investors are willing to spend their money on wind power generation and sign a long-term fixed-price contract [4,5].

The profit maximization approach to electricity market regulation is a strategy that focuses on the potential for market participants to maximize social welfare and production efficiency [6]. With the advent of decentralized power generation and storage systems, there is a clear trend seeing toward increased use of RES [7]. Rising energy demands and a rise in supply has led to an increase in the cost of electricity. This has resulted in a significant loss of revenue for many utilities, which are unable to pass on these costs to their customers [8]. Renewable energy can help utilities meet this challenge by providing them with a reliable source of energy that also helps to reduce maintenance requirements on their equipment such as air pollution control devices (APCDs) [9]. A new study shows that deregulated electricity markets tend to be more profitable for both producers and consumers. This could be because consumers can choose their electricity prices and negotiate with suppliers, whereas producers can work with multiple suppliers and negotiate prices [10]. Energy storage systems allow for the temporary storage of excess energy that can help stabilize prices and make them more predictable [11]. A study by researchers at MIT Technology shows that energy storage systems are a way that allows for the storage of excess electricity from wind farms or solar panels when there's no sun or wind blowing [12].

The world is changing. The era of fossil fuels and centralized power grids is coming to an end, and it will be replaced by a new system in which individuals and communities are empowered to control their own energy needs [13]. This change has been driven by technological innovation, such as battery storage systems, as well as changes in public policy. Storage earns its returns by arbitraging between inter-time differences in the prices of electricity. When storage is present, incumbent businesses bid more fiercely. Energy storage reduces overall system costs and avoids negative real-time profits [14–16].

Using empirical data on the supply and demand for electricity, it has been found that even in marketplaces with a relatively high number of enterprises, the price of energy is far greater than the marginal short-run costs of producing it.. Renewable energy and storage systems using battery are primarily used to optimize system earnings. The goal is to maximize profit from selling power on a market with day-ahead pricing. To maximize energy storage profits and avoid imbalances in supply and consumption, as well as risks in the price fluctuations at nodes caused by congestion of the power grid, a portfolio strategy for financial/physical contract-based energy storage devices has been presented [17–19]. With the use of CAES technology, GENCO is able to employ opportunistic strategies to profit on favorable price variances. The analysis shows that relatively higher amounts of electricity market power induce lower investments in storage capacity, compared to low market power. A robust model with an optimal quadratic cost function for EV charging locations considering RES and storage units has been proposed in Refs. [20–23].

Negative prices are an extreme oversupply of electrical energy, not a good sign of market equilibrium. To reduce peak demand, a wind-pumped storage power system and irrigation system are combined into a probabilistic day-ahead scheduling model. The results of simulations have demonstrated that the proposed approach may successfully increase wind power utilization [24,25]. The results reveal that including the CSP and CAES units into the GENCO's auto-scheduling issue would greatly increase its day ahead market (DAM) profitability [26]. While studying the influence of the storage unit, RFB has been discovered to enhance the performance of the proposed deregulated power system model [27]. Another study proposes reliable, efficient, and effective operational strategies for the combined operation of wind farms and solar PV to optimize financial profit by avoiding imbalance costs [28]. The capacity configuration of CAES systems in the presence

of unreliable wind energy has been studied with historical data using the NSGA-II and TOPSIS optimum selection methods which have shown that a considerable amount of wind abandoning power could be saved each year [29]. The ideal rescheduling of generator output to relieve transmission line congestion is chosen using a genetic algorithm and satisfies the objective function of social welfare maximization by reducing the locational marginal price (LMP) difference between the bus and sub-bus [30].

The ideal location for RES deployment has been determined by the authors of [31,32] using a weighted LMP based method with firefly algorithm (FA) and particle swarm optimization (PSO). Wind and solar plants may optimize their revenue in DAM considering the effect of imbalance costs. After receiving market clearing price (MCP) and market clearing volume (MCV), the market operator uses an AGTO algorithm to rearrange the supplier's bid quantity to enhance societal welfare while satisfying system restrictions. The moth flame optimization (MFO) method is employed for power risk curtailment problems. Investigations are being conducted on how the integration of wind farms affects the system economics in a wind-integrated, deregulated power market. The crowded market-clearing power problem has been dealt with using the generator sensitivity factor (GSF) and the MFO method. The ant lion optimizer (ALO) algorithm is found to be superior to other methods in dealing with the real-time case of wind variation in a modified IEEE 30-bus system [33–38].

The literature review reveals that research has been done on several aspects of a deregulated system associated with wind power and energy storage technologies. However, there were just a few opportunities to investigate the following in this area: (a) What are the implications of adding wind power to both regulated and deregulated electricity networks from an economic and methodological standpoint? (b) How are the system profits affected by the energy market due to imbalance costs? (c) How does the difference in wind speed between the expected and actual wind speed influence the system's profitability? (d) Demand-side bidding's impact on a deregulated electricity market.

In the present work, all the difficulties are inspected, and answers to all these queries very carefully. The following are this work's primary highlights:

- This work relates and differences between regulated and deregulated systems in presence of wind energy in the system.
- In a deregulated power context, a method is developed to examine the effects of the uncertainty of wind speed on the wind-incorporated power system. After the GENCOs and DISCOs adopted a power delivery bond (dependent on a wind speed estimate), if there was any discrepancy between the real and predicted wind speeds, ISO might reward or punish the GENCOs for their excess or deficiency in power supply. Therefore, GENCOs are working to close the power difference between real and predicted wind speed in order to avoid the negative impact of imbalance costs.
- The ESS is the only choice to alleviate this power shortfall. The energy storage systems in a competitive power market can mitigate the power difference and also minimize the burden on thermal power plants, so the financial profit can be exploited.
- The influence of system imbalance cost on the profit is deliberated here for four different locations in India based on the predicted and real wind speed for 24 h.
- A compressed air energy storage (CAES) system has been utilized here to diminish the damaging influences of imbalance costs in the thermal–wind–CAES hybrid system.
- Artificial bee colony algorithms (ABC) and moth flame optimization algorithms (MFO) have been put into action here to check the effectiveness of the proposed method along with sequential quadratic programming (SQP).
- The proportional studies of system risk before and after placement of the CAES system are also illustrated here with different optimization methodologies.
- The effect of imbalance cost has been assessed. The novelty of the work lies in the use of CAES which has been used to maximize the profit by minimizing the effect of imbalance cost which has not been done earlier.

The paper has been divided into few sections. First, the mathematical modeling of the system and constraints have been done. Then objective function has been defined. After that, the proposed methodology and its application have been analyzed. Finally the effects of imbalance cost on the profit of the thermal–wind–CAES hybrid system under consideration have been carried out.

2. Mathematical Modeling

Wind speeds at particular heights, produced wind powers, and wind power investment cost formulations have been utilized here to explore the implications of imbalance cost in a deregulated electrical system.

2.1. Wind Speed Data

Initially, four locations in India were picked at random (Siliguri, Kolkata, Delhi, and Mumbai) to validate the findings using the wind speed information acquired. After this, real-time information of real and predicted wind speeds were collected for the chosen locations at 10 m height. For analysis, the possible wind speed at that specified height was to be calculated (in India, the hub height of the wind turbine is 120 m). The predicted wind speed data for 9th July 2022 was gathered on 10th July 2022 [39]. The real wind speed data for 10th July 2022 was gathered on the 12th of July 2022 [40]. Table 1 exhibits the real and predicted speeds of wind used to explore the outcome of the suggested technique.

Table 1. Predicted wind speed (PWS) and real wind speed (RWS) at 10 m height (in m/s).

Hour	Siliguri		Kolkata		Mumbai		Delhi	
	PWS	RWS	PWS	RWS	PWS	RWS	PWS	RWS
1.	2.50	2.78	3.33	2.22	5.56	5.00	1.94	1.94
2.	2.50	2.22	3.33	2.50	5.28	6.67	2.50	1.94
3.	2.22	1.94	3.33	3.89	5.00	5.00	2.78	2.50
4.	1.94	1.94	3.89	3.06	4.72	6.11	2.50	3.33
5.	1.94	1.94	3.89	3.61	4.17	6.11	2.50	3.89
6.	2.22	2.22	3.89	4.44	3.61	6.11	2.50	2.78
7.	2.22	1.94	4.17	3.61	3.61	4.72	2.78	3.06
8.	1.94	1.67	4.72	5.00	3.61	6.11	2.78	1.94
9.	2.50	1.94	4.72	5.00	3.89	5.56	2.78	2.50
10.	2.50	1.94	4.72	4.17	4.17	6.67	2.50	3.61
11.	2.22	2.50	4.72	5.56	5.00	6.67	2.50	3.61
12.	2.50	2.50	4.72	5.56	5.83	6.11	2.78	2.78
13.	1.94	2.50	5.28	5.00	6.11	5.00	3.06	2.50
14.	1.94	2.22	5.28	4.72	5.00	5.00	3.61	4.17
15.	1.94	1.94	5.28	5.00	5.00	6.67	3.33	3.33
16.	1.94	1.94	5.00	5.28	5.00	5.56	2.78	3.61
17.	2.22	1.94	5.00	5.00	4.72	5.56	2.50	3.33
18.	2.22	1.94	4.72	4.72	4.72	4.72	2.50	4.72
19.	1.94	1.94	4.17	5.56	4.44	5.00	2.78	5.28
20.	1.94	2.22	3.89	4.17	4.17	4.72	3.06	4.17
21.	2.78	1.94	3.61	5.56	4.17	5.56	3.06	2.50
22.	2.78	2.22	3.61	5.56	4.17	5.00	3.06	1.94
23.	2.50	2.78	3.61	5.28	4.44	4.17	3.06	2.50
24.	2.22	2.78	3.61	5.28	4.72	6.67	3.06	2.78

The power law equation [41] was used to compute the wind speed at the height as per requirement:

$$\frac{WS_{dh}}{WS_r} = \left(\frac{h}{10} \right)^N \quad (1)$$

where, ' WS_{dh} ' is the wind speed (at any height ' h '), ' WS_r ' is the reference wind speed (at a height of 10 m') and ' N ' is Hellman's co-efficient. The consideration for this work is $h = 120$ m.

2.2. Wind Power and Wind Power Cost Calculation

The quantity of wind power generated is primarily determined by wind speed, air density, swept area, and turbine efficiency. The wind power (WP) generated can be expressed as follows:

$$P_w = \frac{1}{2} D_a A_T \eta WS_{dh}^3 \quad (2)$$

where, ' D_a ' is the air density (in kg/m^3), ' A_T ' is turbine's swept area in (m^2), η is the efficiency (overall) of the wind plant. In our work considered values are $D_a = 1.225 \text{ kg}/\text{m}^3$, $\eta = 0.49$, and the radius of the turbine rotor (r) = 40 m.

The wind speed database (Table 1) indicates that the wind speed ranges from 1.11 m/s to 6.67 m/s for all the specified sites. According to references [42,43], the cost of investment of a wind power generator is \$3.75/MWh. It is presumed that the power plant will have 50 turbines erected simultaneously. Table 2 quantifies wind speed at the required height, capacity of produced wind power, and wind cost involved for different wind speeds.

Table 2. Wind speed and wind power investment cost.

Sl. No.	Wind Speed at 10 m (m/s)	Wind Speed at 120 m (m/s)	Wind Power with 50 Turbines (MW)	Wind Gen Cost with 50 Turbines (\$/h)
1	1.67	2.38	1.01	3.799
2	1.94	2.77	1.61	6.032
3	2.22	3.17	2.40	9.004
4	2.50	3.57	3.42	12.820
5	2.78	3.96	4.69	17.586
6	3.06	4.36	6.24	23.407
7	3.33	4.75	8.10	30.389
8	3.61	5.15	10.30	38.637
9	3.89	5.55	12.87	48.257
10	4.17	5.94	15.83	59.353
11	4.44	6.34	19.21	72.033
12	4.72	6.73	23.04	86.401
13	5.00	7.13	27.35	102.563
14	5.28	7.53	32.17	120.624
15	5.56	7.92	37.52	140.690
16	5.83	8.32	43.43	162.866
17	6.11	8.72	49.94	187.258
18	6.67	9.51	64.83	243.112

2.3. Modeling of the CAES System

A CAES device is considered to stabilize wind power unpredictability at a constant level in a wind-combined system due to wind speed uncertainty. A CAES has three operational modes: turbine, compressor and idle. When electricity demand is at its peak but wind turbines are not enough to meet the demand, CAES operates in turbine mode. When wind power availability is enough to meet the power requirement, the compressor mode is activated. In the predicted market crisis, the wind farm is expected to retain bargaining power [44]. If there is an excess or deficiency of wind power in the system, the CAES will activate to take care of the situation. The level that the storage tank is filled to determines the CAES system's functioning and is represented by the mathematical expression:

$$\chi_{gt} = \chi_{g0} + P_{e(c)} \eta_c t_{c(c)} - \frac{P_{e(t)} t_{c(t)}}{\eta_t} \quad (3)$$

$$\chi_{g(in)} = P_{e(c)} \eta_c t_{c(c)} \quad (4)$$

$$\chi_{g(out)} = \frac{P_{e(t)} t_{c(t)}}{\eta_t} \quad (5)$$

$$\gamma = \eta_c \eta_t \quad (6)$$

$$\chi_{g(min)} \leq \chi_{gt} \leq \chi_{g(max)} \quad (7)$$

where, $P_{e(c)}$ is the power consumption of CAES (i.e., electric power of the compressor) while charging, $P_{e(t)}$ is electric power generation of CAES (i.e., the electric power of the turbine) while discharging, η_c is compressor efficiency and η_t is the efficiency of the turbine.

In a competitive energy market, the given approach is employed to alleviate system congestion and evaluate the influence of the same on the market-clearing price. In order to calculate the MCP in the energy market, ISO considers bids from both the generator and the consumer ends, and then chooses the MCP in a way that benefits both market participants economically. The following factors are used for each supplier's bid price:

$$BP_{i(t)} = \max\left(\frac{d}{dp} C_i P_{i(t)}\right) \forall i \in G, \forall t = 1 : T \quad (8)$$

where, $C_i P_{i(t)}$ is the i -th generator's cost curve at time t . Additionally, $C_i P_{i(t)}$ is expressed as:

$$C_i P_{i(t)} = \alpha P_{i(t)} + \frac{1}{2} \beta (P_{i(t)})^2 \quad \forall i \in G, \forall t = 1 : T \quad (9)$$

2.4. Locational Marginal Pricing (LMP)

By taking into consideration and calculating transmission congestion and energy pricing, LMP is a technique for determining the delivered energy price at a certain location. This method, commonly referred to as "Nodal Pricing", determines market clearing prices for multiple nodes on a transmission grid. The sum of the marginal costs of generation, transmission losses and line congestion is effectively the locational marginal price at a node.

$$LMP = MC_G + MC_L + MC_{TC} \quad (10)$$

where, MC_G = Marginal cost (generation), MC_L = Marginal cost (losses) and MC_{TC} = Marginal cost (transmission congestion).

2.5. Power Pool

This sort of market model is used by both GENCOs and DISCOs. With the intention of contributing to the pool, GENCOs enter the pool with their highest producing capacity and submit a pricing proposal for transferring the power. The receiving power pricing function, as well as the maximum demand capacity that DISCOs desire to obtain from the pool, are also included in the bids. All buses' power usages and generations are determined by the ISO after social welfare optimization [45]. Let the vector of the active power generation in the pool be:

$$APG_P = [APG_{P,i}; i = 1, 2, 3, \dots \dots T_g] \quad (11)$$

and the vector of the active power demand in the pool is:

$$APL_P = [APL_{P,j}; j = 1, 2, 3, \dots \dots T_d] \quad (12)$$

Therefore, the total active power generation and demand vector is given by

$$APG_T = [APG_{T,i}; i = 1, 2, 3, \dots \dots T_g] \quad (13)$$

$$APL_T = [APL_{T,j}; j = 1, 2, 3, \dots \dots T_d] \quad (14)$$

Here, ' T_g ' is the total number of generators and ' T_d ' is the total number of loads.

2.6. Value-at-Risk (VaR) and Conditional Value-at-Risk (CVaR)

The need for risk management is growing in importance in today’s cutthroat market-place. The risk management area has given significant prominence to the VaR and CVaR approaches. These instruments are founded on probabilistic analysis and assurance level confidence. The confidence threshold for investigating VaR and CVaR values is typically 95%, 98%, and 99%. VaR therefore portrays the least loss with a loss quantity of $(1-\omega)$ percentile, while CVaR demonstrates the typical loss mechanism in the lower tail of the loss distribution. (as shown in Figure 1).

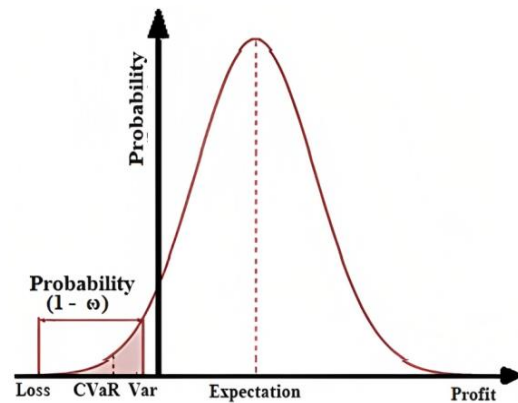


Figure 1. CVaR and VaR representation.

Here, ω is the confidence level, and $g(x,y)$ is the loss associated with the decision vector Q , which is selected from a subset x of \dot{R} . The random vector y in \dot{R} . The probability of $g(x,y)$ is denoted by $p(y)$ which is not exceeding a threshold value of ζ [35]:

$$\psi(x, \zeta) = \int_{g(x,y) \leq \zeta} p(y) dy \tag{15}$$

The formulation of the assurance level based on the risk parameters is as follows:

$$\zeta_\omega(x) = \min\{\zeta \in \dot{R} : \psi(x, \zeta)\} \tag{16}$$

$$\varphi_\omega(x) = \frac{1}{1-\omega} \left[\left(\sum_{j=1}^{j_\omega} p_j - \omega \right) a_{j_\omega} + \sum_{j=j_\omega}^T p_j a_j \right] \tag{17}$$

Here, T is the trials number, which was created under many circumstances, and loss points are ordered as $a_1 < a_2 < a_3 \dots \dots < a_T$.

3. Objective Function

Here an assumption has been taken for an electrical system with ‘ T_b ’ buses, ‘ T_d ’ loads, and ‘ T_g ’ generators. The suggested strategy’s objective function is to examine the influence of variations in predicted and real wind speeds in a wind–thermal hybrid power system operating in a competitive power system. The key parameter of the effect evaluation has likewise been the system profit. The entire system profit is calculated by evaluating the revenue cost, charge rate (both surplus and deficit), imbalance cost, and investment cost of wind power.

The objective of this work is to maximize societal benefit and financial gain while minimizing generation costs and system risk in the event of cost imbalances. The concept of imbalance cost must be considered for performance analysis for any renewable integrated power system. However, based on the author’s knowledge, very limited researchers have considered this concept. The positive imbalance cost provides more system profit, and the negative imbalance cost provides less profit due to the presence of rewards and penalties in the system simultaneously, which are applied to generation companies by the system operators. In this work, the first objective function is the maximization problem and the

second one is the minimization. Mathematically, the objective functions are presented as follows:

First Part of the Objective Function:

$$P_m(t) = TR_m(t) + IMC_m(t) - TGC_m(t) \quad (18)$$

where, $P_m(t)$ = the m-th unit's total profit at time 't'. $TR_m(t)$ = total revenue. $IMC_m(t)$ = total imbalance cost. $TGC_m(t)$ = total generation cost (combining investment costs for wind power and thermal unit generating costs).

Under the new deregulated power situation, the imbalance cost (out of revenue, imbalance and total generating cost) is the most important factor in maximizing the wind-thermal power plant's profit. The total revenue, imbalance cost, and generating cost equations are described as below:

$$TR_m(t) = \sum_{i=1}^{T_g} P_{i,a}(t) \cdot LMP_i(t) \quad (19)$$

$$IMC_m(t) = \sum_{i=1}^{T_g} \left[CR_s(t) + CR_d(t) \cdot \left(\frac{P_{i,f}(t)}{P_{i,a}(t)} \right)^2 \right] \cdot [P_{i,a}(t) - P_{i,f}(t)] \quad (20)$$

where, $P_{i,a}(t)$ = power generated with real wind speed at time 't' at i-th generation bus. $P_{i,f}(t)$ = power generated with predicted wind speed. $CR_s(t)$ = charge rate (surplus) at time 't'. $CR_d(t)$ = charge rate (deficit) at time 't'.

$$TGC_m(t) = GC_m(t) + WGC_m(t) \quad (21)$$

where, WGC = wind power investment cost. The wind-generated power is computed on the basis of predicted wind speed and committed in a DAM arrangement. In reality, the real wind speed data differ from the predicted ones, then the CAES uses them to mitigate this difference in power for its operation to compensate for the difference. However, the discrepancy between the predicted and real wind speed can result in imbalance costs. Equation (20) represents the imbalance cost. The following formulas give how the charge rates (deficit and excess) are calculated:

$$CR_d(t) = (1 + \sigma) \cdot LMP_i(t), \quad CR_s(t) = 0 \text{ when } P_{i,a}(t) < P_{i,f}(t) \quad (22)$$

$$CR_s(t) = (1 - \sigma) \cdot LMP_i(t), \quad CR_d(t) = 0 \text{ when } P_{i,a}(t) > P_{i,f}(t) \quad (23)$$

$$CR_s(t) = CR_d(t) \text{ when } P_{i,a}(t) = P_{i,f}(t) \quad (24)$$

$$GC_m(t) = \sum_{i=1}^{T_g} x + y \cdot P_{i,a}(t) + z \cdot P_{i,a}^2(t) \quad (25)$$

where, $LMP_i(t)$ = LMP at time 't' at i-th bus. $GC_m(t)$ = Power generation cost of the thermal unit. x, y, z are coefficients of generation cost. According to Equation (21), total generation cost consists of two components: thermal system generation cost and wind generation cost. The thermal power system's generation cost is defined using real power generation and the coefficient of generation cost. The imbalance cost coefficient, referred to as ' σ ', is expressed as the ratio of ICR, i.e., the imbalance charge rate (surplus or deficit) to MCP. The ' σ ' varies in the range between 0 to 1. In this work, the value of ' σ ' is assumed to be 0.9.

Second Part of the Objective Function:

$$\text{Min. } \zeta_\omega(x) = \min \left\{ \zeta \in \dot{R} : \psi(x, \zeta) \right\} \quad (26)$$

$$\text{Min. } \varphi_\omega(x) = \frac{1}{1 - \omega} \left[\left(\sum_{j=1}^{j_\omega} p_j - \omega \right) a_{j_\omega} + \sum_{j=j_\omega}^T p_j a_j \right] \quad (27)$$

VaR and CVaR's respective functions are shown in Equations (26) and (27). This is the minimization problem. It is evident that system risk has an inverse relationship with VaR and CVaR, which implies that the system's risk will be at its highest or lowest values if VaR and CVaR have the lowest or highest negative values, respectively. It is thus required to reduce the system's risk to move from the left tail to the right tail of the curve (shown in Figure 1) or to increase the value of VaR and CVaR in a positive direction. Minimizing the cost of system generation is one of this work's primary objectives. The VaR and CVaR have their largest values at the rightmost tail of the curve, when profit of the system is maximum and system generation cost is minimal. As a result, the relationship between the system generation cost and the VaR and CVaR is inverse. However, social welfare is negatively correlated with system-generating costs, meaning that social welfare increases when generation costs are minimized and vice versa. As a result, it may be said that the VaR and CVaR directly relate to social welfare.

3.1. Constraints

The optimum power flow problem was solved using the constraints listed below.

3.1.1. Constraints on Equality

The equality constraint is composed of two components: the real power balancing equation and the power flow equation.

Equations for real power balance:

$$\sum_{i=1}^{T_g} P_{g,i} + WP - P_{loss} - P_d = 0 \quad (28)$$

$$P_{loss} = \sum_{j=1}^{N_{TLN}} G_{ij} \left[|V_i|^2 + |V_j|^2 - 2|V_i||V_j|\cos(\delta_i - \delta_j) \right] \quad (29)$$

where, $P_{g,i}$ = generated power at i -th generating unit, WP = wind power, P_{loss} = transmission loss, P_d = demand in power, N_{TLN} = overall system transmission lines count, G_{ij} = The line conductance between buses ' i ' and ' j ', $|V_i|$, δ_i = magnitude and angle of voltage of bus ' i ', $|V_j|$, δ_j = magnitude and angle of voltage of bus ' j '.

Equations for power flow:

$$P_i - \sum_{k=1}^{T_b} |V_i V_k Y_{ik}| \cos(\theta_{ik} - \delta_i + \delta_k) = 0 \quad (30)$$

$$Q_i + \sum_{k=1}^{T_b} |V_i V_k Y_{ik}| \sin(\theta_{ik} - \delta_i + \delta_k) = 0 \quad (31)$$

where, P_i = real power injected into the system at the bus ' i ', Q_i = reactive power injected into the system at the bus ' i ', Y_{ik} , θ_{ik} = magnitude and angle of the element of i -th row and k -th column of the bus admittance matrix.

3.1.2. Constraints on Inequality

This section contains a variety of continuous and discrete restrictions. These limitations are employed in the optimum power flow to ensure system security and operating limits.

$$V_{i,min} \leq V_i \leq V_{i,max} \text{ where } i = 1, 2, 3, 4, \dots, T_b \quad (32)$$

$$\varphi_{i,min} \leq \varphi_i \leq \varphi_{i,max} \text{ where } i = 1, 2, 3, 4, \dots, T_b \quad (33)$$

$$LF_l \leq LF_l^{max} \text{ where } l = 1, 2, 3, 4, \dots, N_{TLN} \quad (34)$$

$$PG_{i,min} \leq PG_i \leq PG_{i,max} \text{ where } i = 1, 2, 3, 4, \dots, T_b \quad (35)$$

$$QG_{i,min} \leq QG_i \leq QG_{i,max} \text{ where } i = 1, 2, 3, 4, \dots, T_b \quad (36)$$

where, $V_{i,min}$ = bus ' i 's lower voltage limit, $V_{i,max}$ = bus ' i 's upper voltage limit, $\varphi_{i,min}$ = lower angle limit corresponding to the voltage of bus ' i ', $\varphi_{i,max}$ = upper angle limit corresponding to

the voltage of bus ' i ', LF_l = actual line flow of line ' l ', LF_l^{max} = Line ' l 's maximum line flow limit, $PG_{i,min}$ = bus ' i 's lower real power limit, $PG_{i,max}$ = bus ' i 's maximum real power limit, $QG_{i,min}$ = lower reactive power limit of bus ' i ', $QG_{i,max}$ = maximum reactive power limit of bus ' i '.

4. Proposed Method

This work presents a method for assessing the effect of a discrepancy between predicted and real wind speeds in wind-integrated competitive systems over 24 h. The deficit and surplus rates are determined for each case, and the overall imbalance cost is calculated appropriately. The whole recommended strategy is depicted in Figure 2 in form of a flow chart. The GENCOs profit was computed using the actual wind speed using the method. The OPF problem was addressed by rescheduling generators and minimizing total generating cost utilizing the restrictions (Equations (28)–(36)). Furthermore, wind generators were installed in the system under consideration, and the imbalance cost and profit for each wind speed have been deliberated. Here, ' Hr ' is the hour number, ' P_m ' is the total profit, and ' P ' is the profit for a particular hour.

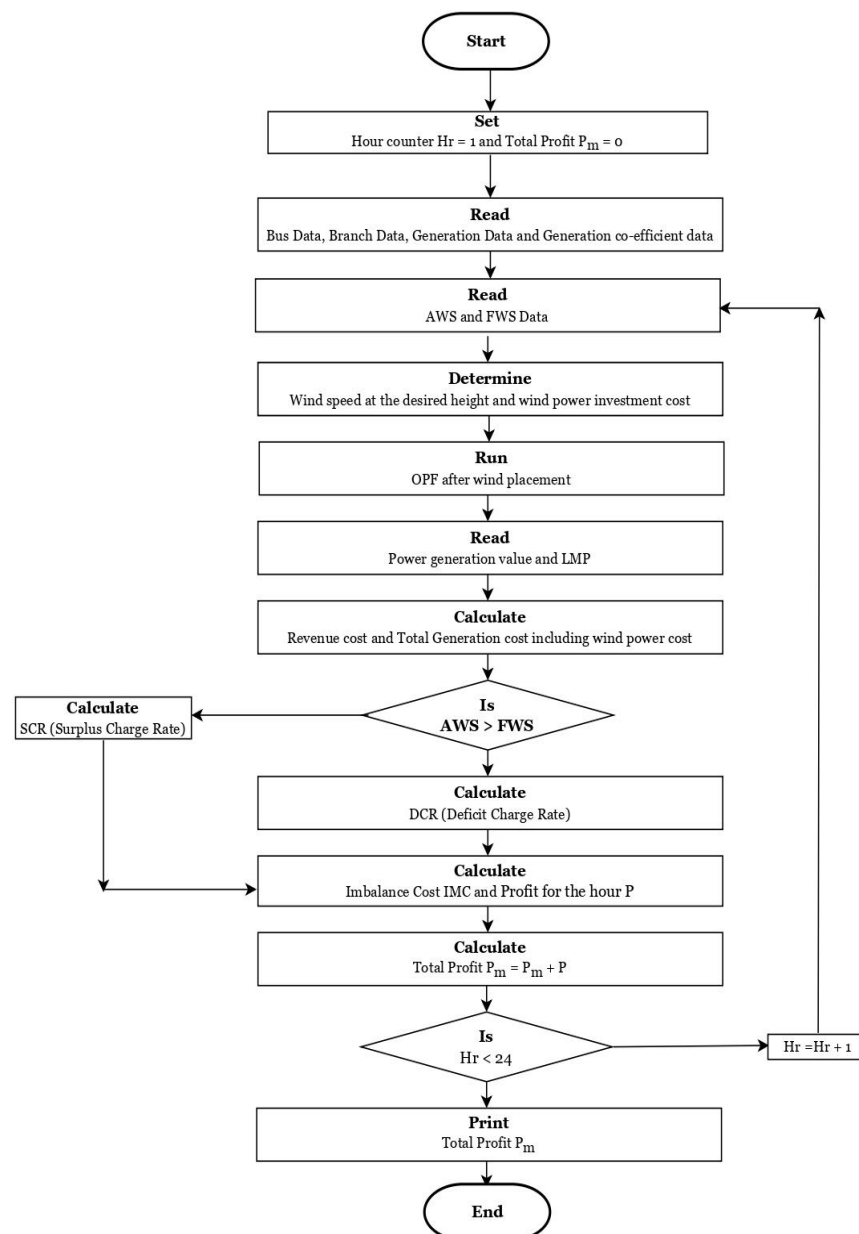


Figure 2. Flowchart of the presented method.

5. Application of the Suggested Approach

To explore the effect of the suggested technique, a modified IEEE 30-bus system was used in this study. In the modified IEEE 30-bus system, there are 30 buses, 6 generators, 41 transmission lines, and 19 loads. The information for the test system is obtained from [46]. To address the optimal power flow problem, SQP was employed at the first stage and afterwards, a few metaheuristic optimization methods were applied to conduct the comparative studies of system performance.

The following systems were considered for the study:

- Regulated system;
- Deregulated system with single auction bidding;
- Deregulated system with double auction bidding.

Case 1: Performance of the System for Single Auction Bidding Prior to Wind Installation

Initial efforts focused on determining the optimal power flow in a system with single auction bidding but no wind generation. In this scenario, the generation cost is 8602.87 \$/h, while the revenue is 10,996.74 \$/h as shown in Table 3. Table 3 also displays the power-generating capacity of each generator, as well as the related LMP at the generator buses.

Table 3. Revenue and generating costs with a single auction bidding system without WF.

	Generation (MW)	LMP (\$/MW)	Generation Cost (\$/h)	Revenue Cost (\$/h)
Gen 1 (Bus 1)	212.25	36.414	8602.87	10,996.74
Gen 2 (Bus 2)	36.23	38.115		
Gen 3 (Bus 5)	29.36	40.587		
Gen 4 (Bus 8)	12.93	40.259		
Gen 5 (Bus 11)	4.36	40.087		
Gen 6 (Bus 13)	0	39.651		

Case 2: System Performance Prior to Wind Installation and When Double Auction Bidding Is Present

In this situation, OPF was addressed without the use of wind power considering the double auction bidding. The generating cost of this system is 7896.03 \$/h as shown in Table 4. Demand side bidding was performed on buses 4 and 21 of the system. This work assessed both generation and demand side biddings to give flexibility to the load and generation sides. Figure 3 depicts a single-line diagram of a modified IEEE 30-bus system with bidding representations. The revenue cost of this example is determined to be 10,321.36 \$/h for a modified IEEE 30-bus system. The generating cost and revenue cost are both decreased following the double auction bidding, as can be shown by looking at the data in Tables 3 and 4.

Table 4. Revenue and generating costs with a double auction bidding without WF.

	Generation (MW)	LMP (\$/MW)	Generation Cost (\$/h)	Revenue Cost (\$/h)
Gen 1 (Bus 1)	210.86	36.207	7896.03	10,321.36
Gen 2 (Bus 2)	36	37.998		
Gen 3 (Bus 5)	26.04	40.521		
Gen 4 (Bus 8)	6.57	40.131		
Gen 5 (Bus 11)	0	39.841		
Gen 6 (Bus 13)	0	39.528		

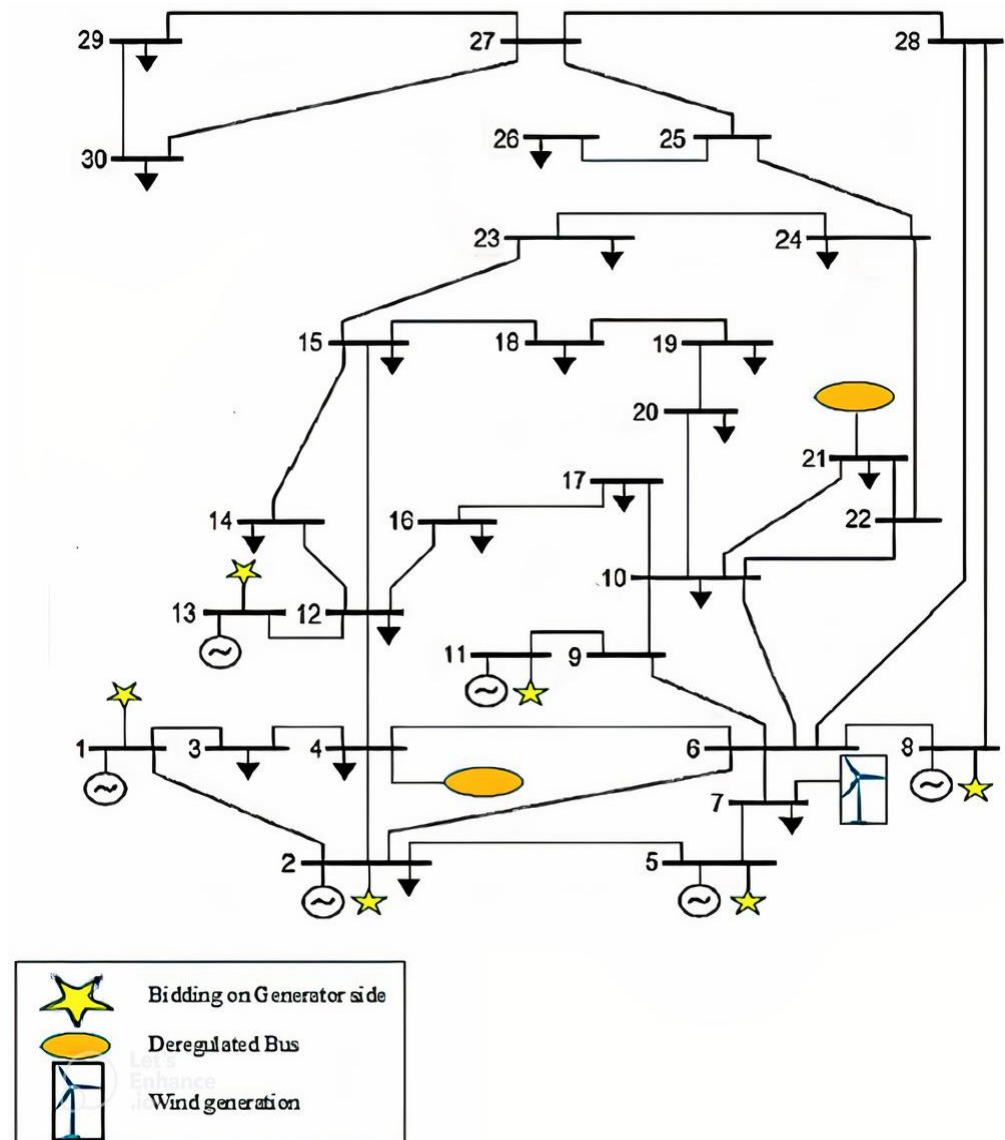


Figure 3. Single line diagram of modified IEEE 30-bus system.

Case 3: System Performance under Double Auction Bidding and Wind Positioning

The location of a wind generator in the investigated system solved the best power flow in this scenario. The wind generator is located on bus 7. In the system, the wind generator was placed at random. After the wind generator was erected, the thermal system's generation cost was computed together with the total generating cost while taking the wind power investment cost into consideration. The total revenue cost has also been estimated using the Equation (19). With winds ranging from 1.11 m/s to 6.67 m/s, Table 5 shows the income and total generating costs for a modified IEEE 30-bus system. According to Table 5, when wind speed increases, the overall generation cost decreases while profit increases.

Table 5. Calculation of revenue and generating costs with wind integration.

Sl. No.	Wind Speed (m/s)	Revenue (\$/h)	Generation Cost (\$/h)	Profit (\$/h)
1.	1.67	10,327.831	7859.009	2468.823
2.	1.94	10,330.800	7837.002	2493.797
3.	2.22	10,335.824	7808.064	2527.760
4.	2.50	10,342.368	7770.710	2571.657
5.	2.78	10,350.565	7724.246	2626.319
6.	3.06	10,360.481	7667.597	2692.884
7.	3.33	10,372.007	7599.679	2772.328
8.	3.61	10,385.406	7519.427	2865.979
9.	3.89	10,400.933	7425.817	2975.116
10.	4.17	10,418.721	7318.183	3100.538
11.	4.44	10,441.601	7195.533	3246.068
12.	4.72	10,475.785	7056.871	3418.914
13.	5.00	10,520.177	6901.293	3618.885
14.	5.28	10,570.406	6727.894	3842.512
15.	5.56	10,625.454	6536.160	4089.294
16.	5.83	10,685.383	6325.256	4360.127
17.	6.11	10,749.535	6093.968	4655.567
18.	6.67	10,542.761	5573.142	4969.620

5.1. Profit Evaluation in a Modified IEEE 30-Bus System

Each time the OPF is run at a different wind speed, the results are documented along with the generating capacity and LMP. This system was used to test the recommended method for a modified IEEE 30-bus system in three situations: (a) calculations for each generator bus’s individual generation and LMP; (b) calculations of the imbalance cost; (c) and the total system’s profit.

5.1.1. Generation and LMP Calculation

In this case, the wind generator was positioned on bus number 7, and OPF was carried out for each wind speed data while taking into account all of the constraints listed in equations Equations (28)–(36). Due to generating rescheduling, the thermal system’s generation cost varies in every situation. Table 6 demonstrates that when wind speed/wind power increases, thermal unit production declines. The value of wind energy has increased, and LMP has also improved. As a consequence, wind power is improved while the cost of producing thermal electricity is decreased in all scenarios. Figures 4 and 5 can be used to compare.

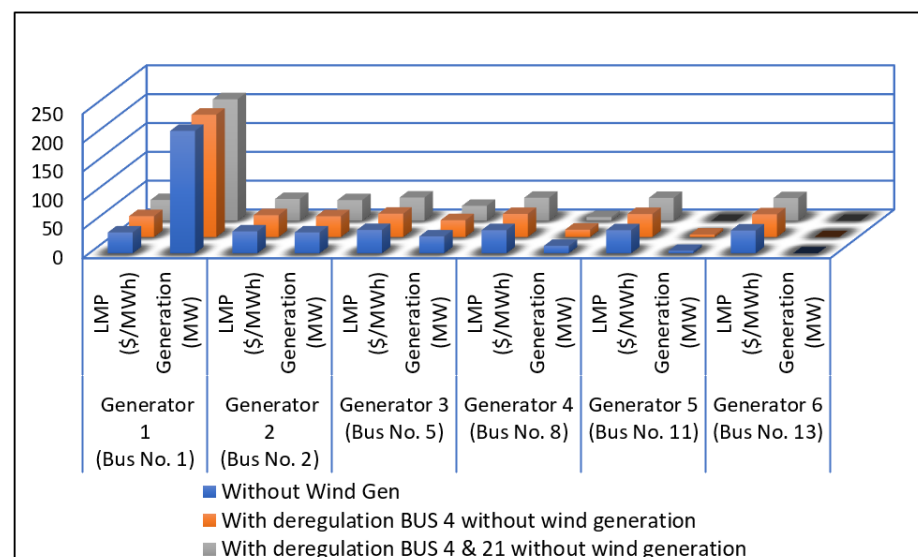


Figure 4. Generation (in MW) and LMP (in \$/MWh) without wind placement.

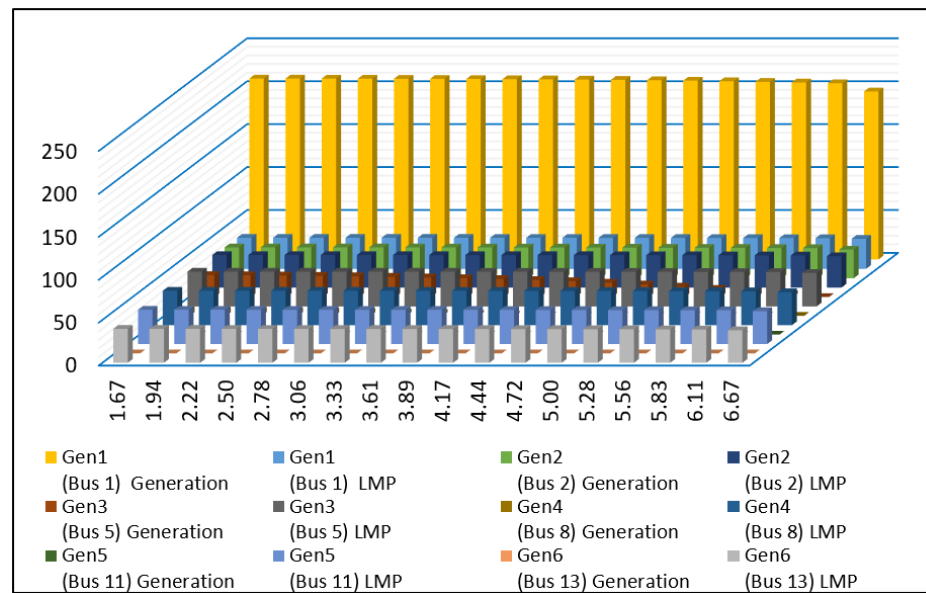


Figure 5. Generation (in MW) and LMP (in \$/MWh) after wind placement.

Table 6. Generation and LMP calculation of modified IEEE 30-bus system after WF placement.

Wind Speed (m/s)	Gen1 (Bus 1)		Gen2 (Bus 2)		Gen3 (Bus 5)		Gen4 (Bus 8)		Gen5 (Bus 11)		Gen6 (Bus 13)	
	Generation (\$)	LMP (\$/MWh)	Generation (\$)	LMP (\$/MWh)	Generation (\$)	LMP (\$/MWh)	Generation (\$)	LMP (\$/MWh)	Generation (\$)	LMP (\$/MWh)	Generation (\$)	LMP (\$/MWh)
1.67	210.78	36.20	35.98	37.99	25.65	40.51	6.24	40.13	0.00	39.88	0.00	39.52
1.94	210.73	36.20	35.97	37.99	25.41	40.51	6.04	40.12	0.00	39.83	0.00	39.51
2.22	210.66	36.19	35.96	37.98	25.11	40.50	5.78	40.12	0.00	39.82	0.00	39.51
2.50	210.58	36.19	35.95	37.97	24.71	40.49	5.45	40.11	0.00	39.81	0.00	39.50
2.78	210.48	36.18	35.93	37.97	24.22	40.48	5.04	40.10	0.00	39.80	0.00	39.48
3.06	210.36	36.17	35.91	37.95	23.62	40.47	4.53	40.09	0.00	39.79	0.00	39.47
3.33	210.21	36.16	35.88	37.94	22.90	40.46	3.93	40.08	0.00	39.78	0.00	39.45
3.61	210.03	36.14	35.85	37.92	22.05	40.44	3.21	40.06	0.00	39.76	0.00	39.43
3.89	209.82	36.13	35.81	37.91	21.06	40.42	2.38	40.05	0.00	39.74	0.00	39.41
4.17	209.58	36.11	35.77	37.88	19.91	40.40	1.43	40.03	0.00	39.72	0.00	39.38
4.44	209.28	36.09	35.72	37.86	18.55	40.37	0.50	40.00	0.00	39.69	0.00	39.34
4.72	208.85	36.05	35.64	37.82	16.78	40.34	0.05	39.95	0.00	39.64	0.00	39.29
5.00	208.29	36.01	35.54	37.77	14.62	40.29	0.00	39.89	0.00	39.58	0.00	39.22
5.28	207.66	35.96	35.43	37.72	12.19	40.24	0.00	39.81	0.00	39.52	0.00	39.14
5.56	206.96	35.91	35.31	37.66	9.50	40.19	0.00	39.73	0.00	39.45	0.00	39.06
5.83	206.18	35.85	35.18	37.59	6.54	40.13	0.00	39.64	0.00	39.37	0.00	38.96
6.11	205.33	35.78	35.03	37.51	3.28	40.07	0.00	39.53	0.00	39.28	0.00	38.86
6.67	195.70	35.04	33.32	36.66	0.00	39.05	0.00	38.51	0.00	38.27	0.00	37.88

5.1.2. Calculation of Imbalance Cost

The imbalance cost was estimated using the Equations (20) to (23) for each variance in projected and real wind speeds. The system’s imbalance cost represents the difference between predicted and real wind speed data. The imbalance cost (negative) is highest when there is the largest discrepancy between the predicted and real wind speed. A deficit charge rate is obtained when the real wind speed is more than the predicted wind speed, and a surplus charge rate is obtained when the real wind speed is greater than the predicted wind speed. By taking the deficit and excess charge rates into account, we may estimate the total imbalance cost of the electrical system. The imbalance cost is zero if there is no difference between the predicted and real wind speed. Table 7 demonstrates that there is a certain number of hours in city cases where the cost of the imbalance is zero. This is due to the precise estimates of wind speed. Table 7 also shows the 24 h interval system’s imbalance cost for each chosen site in India. The “positive” imbalance cost demonstrates

that GENCOs are valued by ISO in terms of rewards for delivering extra power, in contrast to the “negative” imbalance cost, which suggests that GENCOs are punished by ISO for supplying insufficient power.

Table 7. Imbalance cost (in \$/h) calculation.

Hour	Siliguri	Kolkata	Delhi	Mumbai
1	3.749	−347.793	0.000	−499.464
2	−62.157	−285.583	−110.611	44.064
3	−48.445	10.235	−77.263	0.000
4	0.000	−404.948	11.055	16.452
5	0.000	−156.554	16.314	19.067
6	0.000	10.471	3.749	20.674
7	−48.445	−336.597	4.471	17.305
8	−37.882	8.988	−187.899	20.674
9	−110.611	8.988	−77.263	21.276
10	−110.611	−404.641	14.034	50.203
11	3.073	17.262	14.034	46.100
12	0.000	17.262	0.000	6.860
13	5.225	−237.026	−171.985	−1107.252
14	2.433	−448.376	10.382	0.000
15	0.000	−237.026	0.000	46.100
16	0.000	9.463	12.169	14.258
17	−48.445	0.000	11.055	17.262
18	−48.445	0.000	22.040	0.000
19	0.000	20.387	23.969	14.040
20	2.433	6.541	15.208	12.076
21	−187.899	22.039	−171.985	20.387
22	−139.435	22.039	−282.652	16.939
23	3.749	22.006	−171.985	−199.299
24	6.372	22.006	−94.701	47.895

5.1.3. Profit Estimate for 24 h

The revenue cost and the generating cost are the two main factors that define an electrical system’s profit at any given time. For the purpose of including the imbalance cost variables into the system’s profit calculation, we compared predicted and real wind speeds in this study. In the case of the system operating in an environment with deregulated power, Table 8 shows the profit values for a 24 h period for each site. Profit is increased by reducing the detrimental impact of imbalance costs. After installing the WF in the system and analyzing both anticipated and real wind speed data, it was discovered that Mumbai has the most profit owing to more accurate wind speed forecasting, while Siliguri has the lowest profit due to less precise forecasting.

Table 8. Profit (in \$/h) computation of the system.

Hour	Siliguri	Kolkata	Delhi	Mumbai
1	2630.068	2179.967	2493.797	3119.421
2	2465.603	2286.074	2383.187	5013.683
3	2445.352	2985.351	2494.394	3618.885
4	2493.797	2287.935	2783.383	4672.018
5	2493.797	2709.425	2991.430	4674.634
6	2527.760	3256.539	2630.068	4676.241
7	2445.352	2529.382	2697.354	3436.219
8	2430.940	3627.873	2305.898	4676.241
9	2383.187	3627.873	2494.394	4110.570
10	2383.187	2695.897	2880.013	5019.823
11	2574.730	4106.556	2880.013	5015.720
12	2571.657	4106.556	2626.319	4662.426

Table 8. Cont.

Hour	Siliguri	Kolkata	Delhi	Mumbai
13	2576.883	3381.858	2399.672	2511.633
14	2530.192	2970.538	3110.920	3618.885
15	2493.797	3381.858	2772.328	5015.720
16	2493.797	3851.975	2878.149	4103.552
17	2445.352	3618.885	2783.383	4106.556
18	2445.352	3418.914	3440.954	3418.914
19	2493.797	4109.681	3866.481	3632.925
20	2530.192	3107.078	3115.745	3430.990
21	2305.898	4111.333	2399.672	4109.681
22	2388.325	4111.333	2211.146	3635.823
23	2630.068	3864.518	2399.672	2901.239
24	2632.691	3864.518	2531.618	5017.515

5.2. Profit Comparison after WF Installation, Taking RWS and PWS into Consideration

This case is a summary of the overall outcomes and judgments reached as a consequence of the planned work. Figures 6 and 7 depict a comparison for profit while considering various instances for all selected locations. It is evident that after wind placement, profit is maximized for every location, however, in the case of RWS and PWS both, profit is minimized for every location owing to the presence of imbalance cost. In a deregulated electricity market, contracts between market players must take into account the wind speed since wind flow is unpredictable. However, wind speed prediction gives the system more security and flexibility when using wind power. Profit may be decreased if there is a mismatch between PWS and RWS.

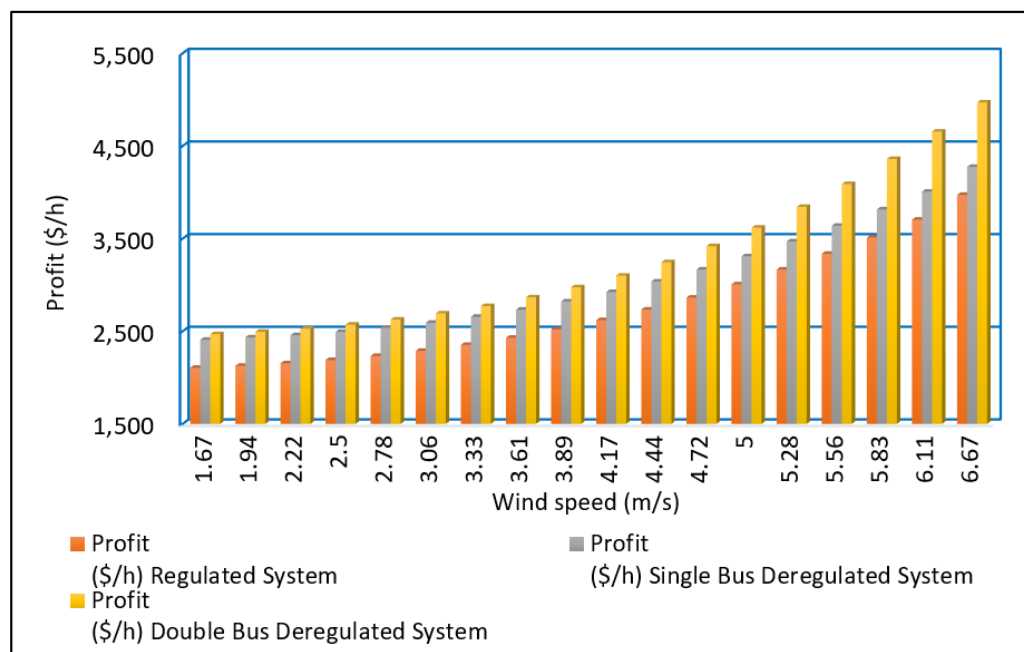


Figure 6. Profit for a regulated and deregulated system after the placement of a wind generator.

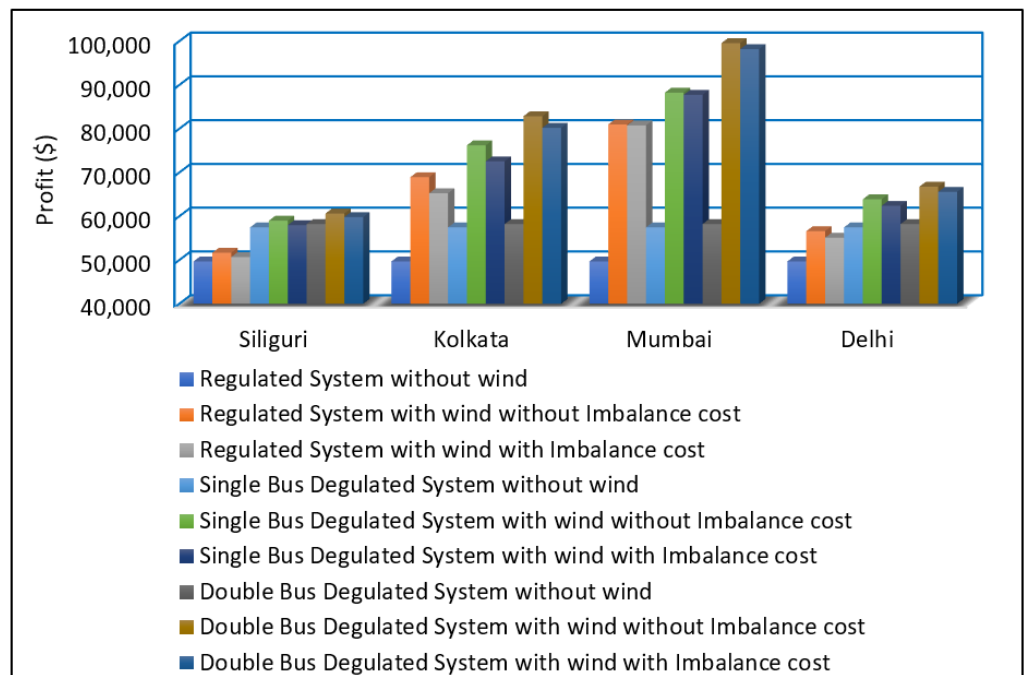


Figure 7. Comparative study of profits (\$) in different locations over 24 h.

Figure 8 compares the average profit for several instances in the modified IEEE 30-bus system. After accounting for both ‘RWS’ and ‘PWS’, Mumbai has obtained the highest average profit, owing to the efficient and secure (i.e., in most cases, the real wind speed is larger than the anticipated one) wind speed forecasting. The lowest average profit is for Siliguri, which is owing to a substantial discrepancy in wind speed predictions.

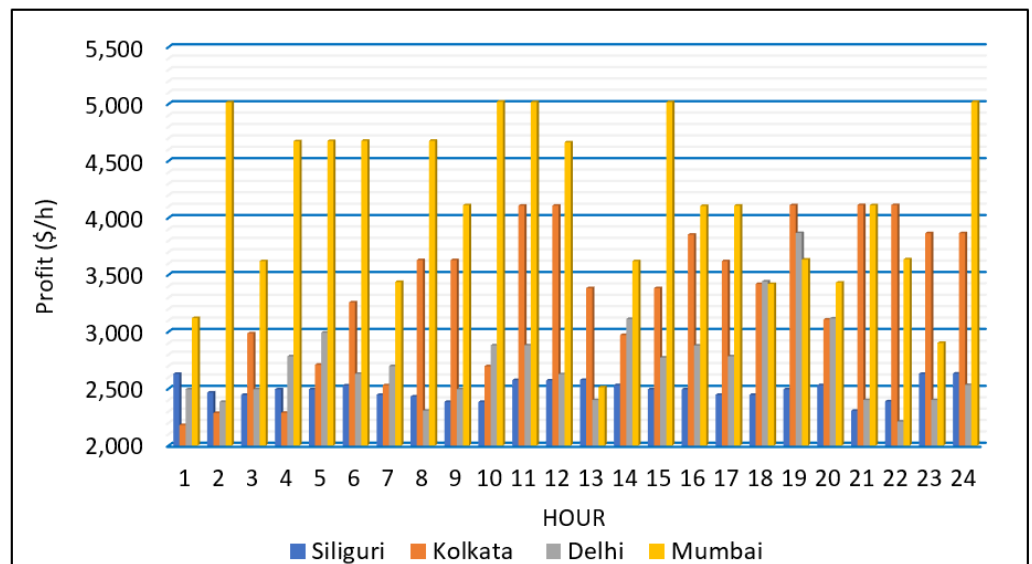


Figure 8. Average profit (\$/h) comparison for 24 h.

5.3. Revenue, Bus Voltage and Imbalance Cost after WF Placement

In a power system, the bus voltage and system economy are very important for the stability of the network. We have analyzed the revenue and bus voltage of the system under consideration for various conditions, i.e., regulated system, single bus deregulated system and double bus deregulated system. Figure 9 shows the healthy condition of the system after the application of the proposed method. Figure 10 depicts the steady improvement in revenue for deregulated systems over the regulated system. Figure 11 gives an overview of

the variation of imbalance costs of different cities under consideration for various cases for 24 h.

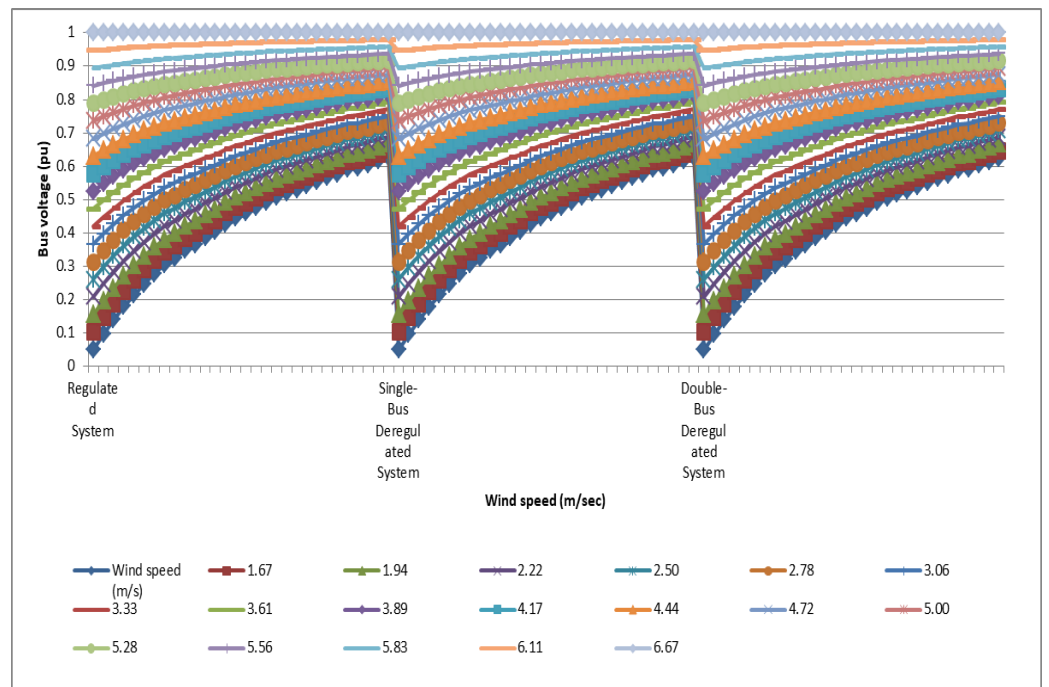


Figure 9. Study of bus voltage for different wind speeds.

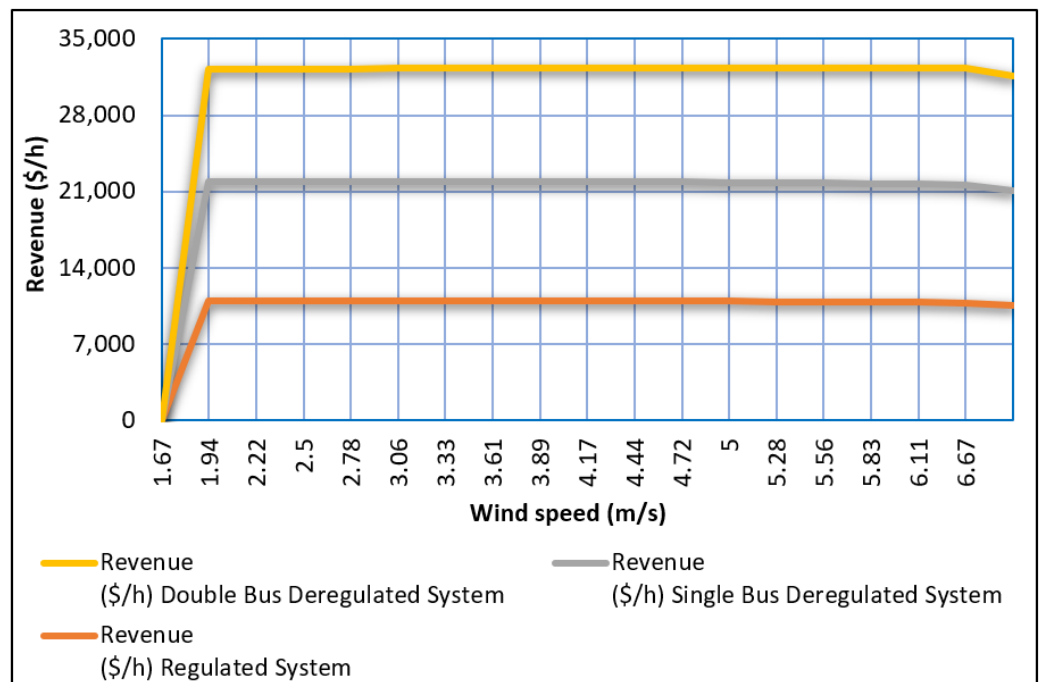


Figure 10. Revenue for regulated and deregulated systems after the placement of a wind generator.

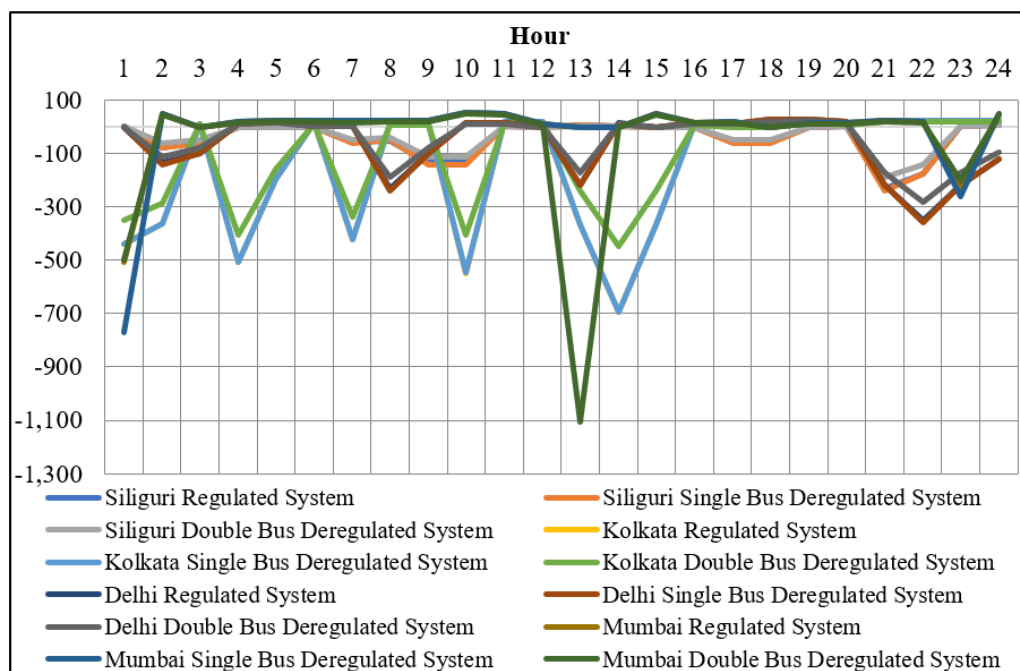


Figure 11. Imbalance cost (\$/h) analysis during 24 h in different cities.

Case 4: system performance with the placement of wind farm and CAES system

The system economic studies with the integration of CAES into the deregulated, wind-integrated power system are presented in this section. It is fairly evident from the previous section that the unfavorable impact of imbalance costs lowers system profit. The problem of imbalance cost can be solved using the installation of the CAES system. During the off-peak load period and the more actual wind power availability cases, the CAES works in charging mode, and during the on-peak load period, the CAES operates in discharging mode. In the on-peak load situation, CAES can inject some extra power into the system and reduce the discrepancy between the real and predicted wind power schedules. A fixed generation capacity of 3 MW by the CAES system has been established at bus 6 in the modified IEEE 30-bus system. The bus was selected for the CAES placement based on the logic of a maximum number of transmission lines connected to that particular bus. To verify the competencies and applicability of the presented method, different optimization algorithms, i.e., ABC and MFO, have been used along with SQP. The controlling parameters of MFO and ABC algorithms have been collected from Refs. [37,46]. Table 9 and Figure 12 display the average hourly profit with different optimization techniques for Siliguri and Delhi.

Table 9. Average hourly profit with different optimization techniques for Siliguri and Delhi.

		Average Hourly Profit (\$/h)			
		Siliguri		Delhi	
Optimization Techniques	Conditions	Regulated System	Deregulated System—Double Bus DSB	Regulated System	Deregulated System—Double Bus DSB
SQP	With WF	2111.360	2492.157	2295.753	2732.083
	With WF and CAES	2113.621	2495.248	2297.547	2735.348
ABC	With WF	2112.367	2493.621	2296.547	2733.217
	With WF and CAES	2114.626	2496.358	2298.315	2736.629
MFO	With WF	2113.455	2494.812	2297.346	2734.328
	With WF and CAES	2115.367	2497.924	2299.532	2736.614

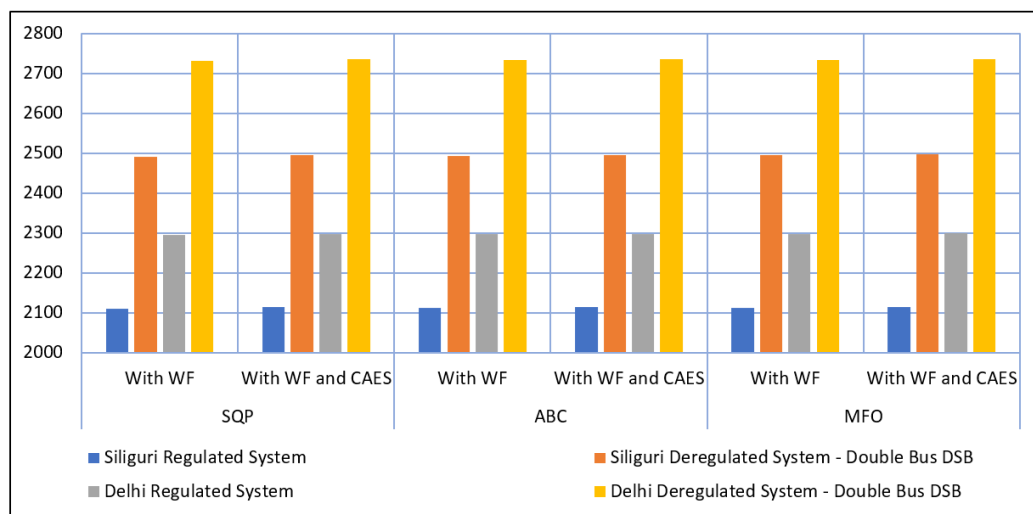


Figure 12. Average hourly profit with different optimization techniques for Siliguri and Delhi.

According to the findings, the placement of CAES alongside wind farms yields higher system profits than the profits obtained in the wind-incorporated electrical system without CAES. The key originality of this paper is the first use of the MFO optimization technique for this kind of economic problem. For all consideration conditions, MFO offers the best results among the three optimization strategies applied in terms of system profit maximization. So, it can be concluded that the CAES placement and application of MFO techniques maximize the system profit in presence of an imbalance cost.

Case 5: System risk Analysis with the placement of wind farm and CAES system

System risk analysis plays an important role in the secure operation of an electrical system. If any faults have occurred in the system, then the fault needs to be removed from the system very quickly, otherwise, there is a chance of system failure. Here, using the risk analysis tools VaR and CVaR, the system risk has been calculated based on the LMP of each bus in the system. A 95% confidence level was used to calculate all of the risk statistics.

Table 10 and Figure 13 display the system risk for Delhi under various system settings using various optimization strategies. It is seen that with the use of MFO algorithms, a maximum number of wind farms can operate with the least amount of system risk. After the CAES system was installed in a deregulated environment, the system risk was reduced. This is happening due to the minimization of load on the grid by providing more power locally.

Table 10. System risk with various optimization methods for Delhi under various system scenarios.

Sl. No.	Wind Power	VaR				CVaR			
		With Wind Farm Using SQP	With Wind Farm-CAES System Using SQP	With Wind Farm-CAES System Using ABC	With Wind Farm-CAES System Using MFO	With Wind Farm Using SQP	With Wind Farm-CAES System Using SQP	With Wind Farm-CAES System Using ABC	With Wind Farm-CAES System Using MFO
1	10.3 MW	-0.4316	-0.4214	-0.4124	-0.4018	-0.5918	-0.5825	-0.5715	-0.5615
2	8.1 MW	-0.4345	-0.4233	-0.4147	-0.4037	-0.5962	-0.5885	-0.5773	-0.5656
3	3.42 MW	-0.4351	-0.4246	-0.4158	-0.4041	-0.5971	-0.589	-0.5764	-0.5667

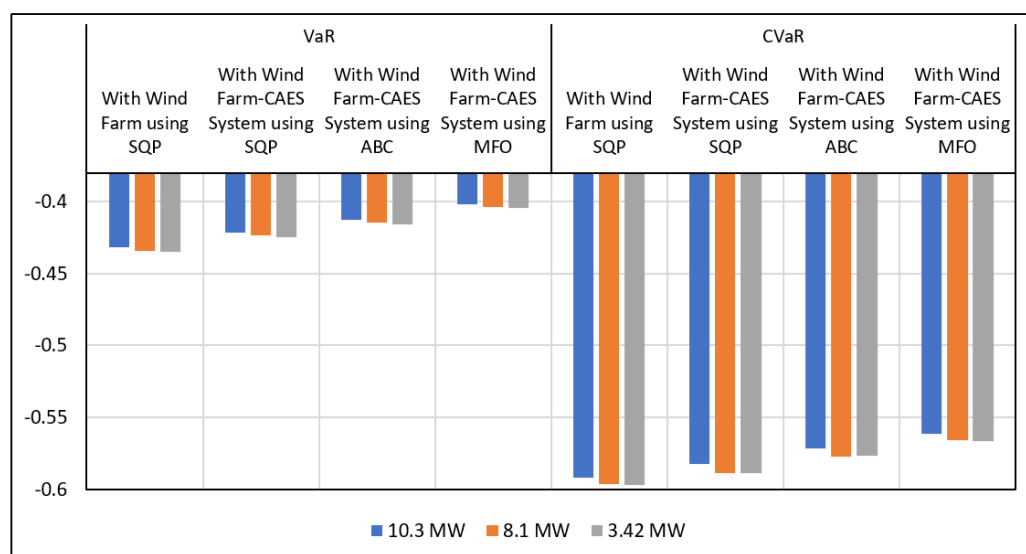


Figure 13. System risk with different optimization techniques for Delhi with different system conditions.

This work can be done using any other standard as well as practical systems. If this work perform in the large system, the economic profit will be greater, and system risk will reduced, after the placement of CAES in the system.

6. Conclusions

This work presents a strategy for measuring the influence of wind speed uncertainty on a wind-integrated electrical system in a competitive double auction power market. The imbalance cost mainly creates problems in the system economy in a renewable integrated power system. This paper presents an optimal operation of the CAES system with the wind farm and thermal power plant to mitigate the negative effect of imbalance cost in the system economy. The CAES provides extra power to the system based on the energy requirement in the grid. The suggested method was tested on a modified IEEE 30-bus system. The test results illustrate the efficiency of the suggested technique in terms of maximizing profit at various locations in India. The impact of a mismatch between forecasted and real wind speeds on a wind-integrated power system has also been evaluated and handled in this work. The notion of power shortfall and surplus utilization has also been presented. The simulation takes into account the fluctuations in wind speed over 24 h. As a consequence, the LMP of the system has been significantly improved by the addition of wind power to the system. The system risk has also reduced after the placement of CAES with WF and thermal power plants, which encourages the power plant developer to invest the money in the installation of the CAES system with renewable plants to minimize the chances of long-term economic losses. This study focused on the CAES system, which is more appropriate because of its enormous storage capacity and quick startup. However, there are several disadvantages to CAES, including as the fact that natural gas must be used to heat the air for the expanding stage and that it is less efficient than alternative storage systems. ABC, MFO, and SQP optimization methods were used to find the best power flow solution and compute profit. When ABC, MFO, and SQP were applied to two locations and the outcomes were compared, it could be observed that MFO performs better in terms of the average profit value. Additionally, it is implied that it will be true for the other two locations also. In the last part, a risk analysis study was conducted using the analysis tools, i.e., VaR and CVaR, with confidence levels of 95% in the wind and pumped hydroelectric storage integrated system. The system risk has been measured based on the LMP of every bus in the system using ABC, MFO, and SQP algorithms. It is clear that MFO performs better in terms of the risk coefficient value, which shows that system risk decreases as wind generation rises. This happens as the wind farms meets part of the local load requirement

resulting reduction in load demand from the grid. The primary originality of this paper is the first use of the MFO algorithm in this kind of research. Assessments have been made on the imbalance cost's impact. The uniqueness of the study consists in the use of CAES, which has never been done before in order to optimize profit by reducing the impact of cost imbalance.

Author Contributions: Conceptualization, M.R.C. and S.D.; methodology, M.R.C., S.D. and J.B.B.; software, M.R.C.; validation, P.K.S. and T.S.U.; formal analysis, S.D.; investigation, M.R.C. and J.B.B.; resources, M.R.C. and S.D.; data curation, P.K.S. and T.S.U.; writing—original draft preparation, M.R.C. and J.B.B.; writing—review and editing, S.D., P.K.S. and T.S.U.; visualization, S.D.; supervision, P.K.S. and T.S.U.; project administration, T.S.U.; funding acquisition, T.S.U. All authors have read and agreed to the published version of the manuscript.

Funding: This research received no external funding.

Institutional Review Board Statement: Not applicable.

Informed Consent Statement: Not applicable.

Data Availability Statement: Not applicable.

Conflicts of Interest: The authors declare no conflict of interest.

Abbreviations and Notations

GENCOs	Generation Companies
TRANSCOs	Transmission Companies
DISCOs	Distribution Companies
APCDs	Air Pollution Control Devices
CAES	Compressed Air Energy Storage
CSP	Concentrated Solar Power
DAM	Day Ahead Markets
RFB	Redox Flow Battery
LMP	Locational Marginal Price
GWO	Grey Wolf Optimization
FA	Firefly Algorithm (FA)
PSO	Particle Swarm Optimization
MCP	Market Clearing Price
MCV	Market Clearing Volume
AGTO	Artificial Gorilla Troops Optimizer
MFO	Moth Flame Optimization
GSF	Generator Sensitivity Factor
ALO	Ant Lion Optimizer
ISO	Independent System Operator
ICR	Imbalance Charge Rate
SQP	Sequential Quadratic Programming
OPF	Optimal Power Flow
RWS	Real Wind Speed
PWS	Predicted Wind Speed
WS_{dh}	wind speed (at any height ' h ')
WS_r	reference wind speed
N	Hellman's co-efficient
D_a	air density
A_T	turbine's swept area in
η	efficiency (overall) of the wind plant
$P_{e(c)}$	power consumption of CAES (i.e., electric power of the compressor) while charging
$P_{e(t)}$	electric power generation of CAES (i.e., the electric power of the turbine) while discharging
η_c	compressor efficiency
η_t	efficiency of the turbine

$C_i P_{i(t)}$	i -th generator's cost curve at time t
MC_G	Marginal cost (generation)
MC_L	Marginal cost (losses)
MC_{TC}	Marginal cost (transmission congestion)
APG_P	vector of the active power generation in the pool
APL_P	vector of the active power demand in the pool
APG_T	total active power generation vector
APL_T	total active power demand vector
T_g	total number of generators
T_d	total number of loads
$P_m(t)$	the m -th unit's total profit at time ' t '
$TR_m(t)$	total revenue
$IMC_m(t)$	total imbalance cost
$TGC_m(t)$	total generation cost
$P_{i,a}(t)$	power generated with real wind speed at time ' t ' at i -th generation bus
$P_{i,f}(t)$	power generated with predicted wind speed
$CR_s(t)$	charge rate (surplus) at time ' t '
$CR_d(t)$	charge rate (deficit) at time ' t '
$LMP_i(t)$	LMP at time ' t ' at i -th bus
$GC_m(t)$	Power generation cost of the thermal unit
$P_{g,i}$	generated power at i -th generating unit
WP	wind power
P_{loss}	transmission loss
P_d	demand in power
N_{TLN}	overall system transmission lines count
G_{ij}	The line conductance between buses ' i ' and ' j '
$ V_i , \delta_i$	magnitude and angle of voltage of bus ' i '
$ V_j , \delta_j$	magnitude and angle of voltage of bus ' j '
P_i	real power injected into the system at the bus ' i '
Q_i	reactive power injected into the system at the bus ' i '
$V_{i,min}$	bus ' i 's lower voltage limit
$V_{i,max}$	bus ' i 's upper voltage limit
$\varphi_{i,min}$	lower angle limit corresponding to the voltage of bus ' i '
$\varphi_{i,max}$	upper angle limit corresponding to the voltage of bus ' i '
LF_l	actual line flow of line ' l '
LF_l^{max}	maximum line flow limit of Line ' l '
$PG_{i,min}$	lower real power limit of bus ' l '
$PG_{i,max}$	maximum real power limit of bus ' l '
$QG_{i,min}$	lower reactive power limit of bus ' i '
$QG_{i,max}$	maximum reactive power limit of bus ' i '

References

1. Gencer, B.; Larsen, E.R.; van Ackere, A. Understanding the coevolution of electricity markets and regulation. *Energy Policy* **2020**, *143*, 111585. [CrossRef]
2. Shahidehpour, M.; Marwali, M. Introduction. In *Maintenance Scheduling in Restructured Power Systems*; The Springer International Series in Engineering and Computer Science; Springer: Boston, MA, USA, 2000. [CrossRef]
3. AL Shaqsi, A.Z.; Sopian, K.; Al-Hinai, A. Review of energy storage services, applications, limitations, and benefits. *Energy Rep.* **2020**, *6* (Suppl. S7), 288–306. [CrossRef]
4. OECD Green Growth Studies, Energy. Available online: <https://www.oecd.org/greengrowth/greening-energy/49157219.pdf> (accessed on 6 August 2022).
5. Kumar, M. Social, Economic, and Environmental Impacts of Renewable Energy Resources. In *Wind Solar Hybrid Renewable Energy System*; IntechOpen: London, UK, 2020. Available online: <https://www.intechopen.com/chapters/70874> (accessed on 6 August 2022). [CrossRef]
6. Bublitz, A.; Keles, D.; Zimmermann, F.; Fraunholz, C.; Fichtner, W. A survey on electricity market design: Insights from theory and real-world implementations of capacity remuneration mechanisms. *Energy Econ.* **2019**, *80*, 1059–1078, ISSN 0140-9883. [CrossRef]
7. Razzaghi Asl, S. Re-powering the Nature-Intensive Systems: Insights From Linking Nature-Based Solutions and Energy Transition. *Front. Sustain. Cities* **2022**, *4*, 91. [CrossRef]

8. Climate Impacts Energy. United States Environmental Protection Agency (EPA). Available online: https://19january2017snapshot.epa.gov/climate-impacts/climate-impacts-energy_html (accessed on 7 August 2022).
9. Abdallah, L.; El-Shennawy, T. Reducing Carbon Dioxide Emissions from Electricity Sector Using Smart Electric Grid Applications. *J. Eng.* **2013**, *2013*, 845051. [[CrossRef](#)]
10. Necoechea-Porras, P.; López, A.; Salazar-Elena, J. Deregulation in the Energy Sector and Its Economic Effects on the Power Sector: A Literature Review. *Sustainability* **2021**, *13*, 3429. [[CrossRef](#)]
11. Das, C.K.; Bass, O.; Kothapalli, G.; Mahmoud, T.S.; Habibi, D. Overview of energy storage systems in distribution networks: Placement, sizing, operation, and power quality. *Renew. Sustain. Energy Rev.* **2018**, *91*, 1205–1230. [[CrossRef](#)]
12. Energy Storage Important to Creating Affordable, Reliable, Deeply Decarbonized Electricity Systems. Available online: <https://news.mit.edu/2022/energy-storage-important-creating-affordable-reliable-deeply-decarbonized-electricity-systems-0516> (accessed on 11 August 2022).
13. Stephens, J.C. Energy Democracy: Redistributing Power to the People Through Renewable Transformation. *Environ. Sci. Policy Sustain. Dev.* **2019**, *61*, 4–13. [[CrossRef](#)]
14. Ugurlu, U.; Tas, O.; Kaya, A.; Oksuz, I. The Financial Effect of the Electricity Price Forecasts' Inaccuracy on a Hydro-Based Generation Company. *Energies* **2018**, *11*, 2093. [[CrossRef](#)] [[PubMed](#)]
15. Liu, J.; Bo, R.; Wang, S.; Chen, H. Optimal scheduling for profit maximization of energy storage merchants considering market impact based on dynamic programming. *Comput. Ind. Eng.* **2021**, *155*, 107212. [[CrossRef](#)]
16. The Economics of Grid-Scale Energy Storage in Wholesale Electricity Markets. Available online: <https://climate.mit.edu/posts/economics-grid-scale-energy-storage-wholesale-electricity-markets#YvDupD370d8.link> (accessed on 8 August 2022).
17. Rudkevich, A.; Duckworth, M.; Rosen, R. Modeling Electricity Pricing in a Deregulated Generation Industry: The Potential for Oligopoly Pricing in a Poolco. *Energy J.* **1998**, *19*. [[CrossRef](#)]
18. Patil, G.S.; Mulla, A.; Dawn, S.; Ustun, T.S. Profit Maximization with Imbalance Cost Improvement by Solar PV-Battery Hybrid System in Deregulated Power Market. *Energies* **2022**, *15*, 5290. [[CrossRef](#)]
19. Lan, P.; Han, D.; Zhang, R.; Xu, X.; Yan, Z. Optimal portfolio design of energy storage devices with financial and physical right market. *Front. Energy* **2022**, *16*, 95–104. [[CrossRef](#)]
20. Siddiqui, A.S.; Sioshansi, R.; Conejo, A.J. Merchant Storage Investment in a Restructured Electricity Industry. *Energy J.* **2019**, *40*, 129–163. [[CrossRef](#)]
21. Kumar, P.; Bharadwaj, S.K. Optimal Bidding Strategies and Profit Maximization for Micro Grid Combinations in Electric Energy Market in Indian Restructured Environment. *Int. J. Adv. Res. Eng. Technol.* **2020**, *11*, 931–949. Available online: <https://ssrn.com/abstract=3658341> (accessed on 22 July 2020).
22. Chen, W.; Tian, Y.; Zheng, K.; Wan, N. Influences of mechanisms on investment in renewable energy storage equipment. *Environ. Dev. Sustain.* **2022**. [[CrossRef](#)]
23. Murphy, C.; Schleifer, A.; Eurek, K. A taxonomy of systems that combine utility-scale renewable energy and energy storage technologies. *Renew. Sustain. Energy Rev.* **2021**, *139*, 110711. [[CrossRef](#)]
24. Li, K.; Cursio, J.D.; Sun, Y.; Zhu, Z. Determinants of price fluctuations in the electricity market: A study with PCA and NARDL models. *Econ. Res.* **2019**, *32*, 2404–2421. [[CrossRef](#)]
25. Zhang, M.; Chen, J.; Yang, Z.; Peng, K.; Zhao, Y.; Zhang, X. Stochastic day-ahead scheduling of irrigation system integrated agricultural microgrid with pumped storage and uncertain wind power. *Energy* **2021**, *237*, 121638. [[CrossRef](#)]
26. Gilvaei, M.N.; Imani, M.H.; Ghadi, M.J.; Li, L.; Golrang, A. Profit-Based Unit Commitment for a GENCO Equipped with Compressed Air Energy Storage and Concentrating Solar Power Units. *Energies* **2021**, *14*, 576. [[CrossRef](#)]
27. Selvaraju, R.K.; Somaskandan, G. Impact of energy storage units on load frequency control of deregulated power systems. *Energy* **2016**, *97*, 214–228. [[CrossRef](#)]
28. Das, S.S.; Das, A.; Dawn, S.; Gope, S.; Ustun, T.S. A Joint Scheduling Strategy for Wind and Solar Photovoltaic Systems to Grasp Imbalance Cost in Competitive Market. *Sustainability* **2022**, *14*, 5005. [[CrossRef](#)]
29. Yu, Q.; Tian, L.; Li, X.; Tan, X. Compressed Air Energy Storage Capacity Configuration and Economic Evaluation Considering the Uncertainty of Wind Energy. *Energies* **2022**, *15*, 4637. [[CrossRef](#)]
30. Eladl, A.; Kaddah, S.; Haikal, E. Optimal generation rescheduling for congestion management, LMP enhancement and social welfare maximization. In Proceedings of the 2017 Nineteenth International Middle East Power Systems Conference (MEPCON), Cairo, Egypt, 19–21 December 2017; pp. 1190–1194. [[CrossRef](#)]
31. Farzana, D.F.; Mahadevan, K. Performance comparison using firefly and PSO algorithms on congestion management of deregulated power market involving renewable energy sources. *Soft Comput.* **2020**, *24*, 1473–1482. [[CrossRef](#)]
32. Gautam, A.; Sharma, P.; Kumar, Y. Mitigating congestion by optimal rescheduling of generators applying hybrid PSO–GWO in deregulated environment. *SN Appl. Sci.* **2021**, *3*, 69. [[CrossRef](#)]
33. Özcan, M.; Keysan, O.; Satır, B. Optimum bidding strategy for wind and solar power plants in day-ahead electricity market. *Energy Syst.* **2021**, *12*, 955–987. [[CrossRef](#)]
34. Kumar, K.K.P.; Soren, N.; Latif, A.; Das, D.C.; Hussain, S.M.S.; Al-Durra, A.; Ustun, T.S. Day-Ahead DSM-Integrated Hybrid-Power-Management-Incorporated CEED of Solar Thermal/Wind/Wave/BESS System Using HFPSO. *Sustainability* **2022**, *14*, 1169. [[CrossRef](#)]

35. Singh, N.K.; Koley, C.; Gope, S.; Dawn, S.; Ustun, T.S. An Economic Risk Analysis in Wind and Pumped Hydro Energy Storage Integrated Power System Using Meta-Heuristic Algorithm. *Sustainability* **2021**, *13*, 13542. [[CrossRef](#)]
36. Patil, G.S.; Mulla, A.; Ustun, T.S. Impact of Wind Farm Integration on LMP in Deregulated Energy Markets. *Sustainability* **2022**, *14*, 4354. [[CrossRef](#)]
37. Dawn, S.; Gope, S.; Das, S.S.; Ustun, T.S. Social Welfare Maximization of Competitive Congested Power Market Considering Wind Farm and Pumped Hydroelectric Storage System. *Electronics* **2021**, *10*, 2611. [[CrossRef](#)]
38. Gope, S.; Dawn, S.; Das, S.S.; Galiveeti, H.R. Wind farm integrated restructured electricity market analysis using Ant Lion optimizer algorithm. *Energy Sources Part A Recovery Util. Environ. Eff.* **2021**. [[CrossRef](#)]
39. India Meteorological Department, Ministry of Earth Sciences, Government of India. AWS Lab, Pune. Available online: <http://www.imd.gov.in/Welcome%20To%20IMD/Welcome.phpandhttp://www.imdaws.com/ViewAwsData.aspx> (accessed on 10 July 2022).
40. Database: World Temperatures-Weather around the World. Available online: www.timeanddate.com/weather (accessed on 12 July 2022).
41. Dawn, S.; Tiwari, P.K.; Goswami, A.K. An approach for efficient assessment of the performance of double auction competitive power market under variable imbalance cost due to high uncertain wind penetration. *Renew. Energy* **2017**, *108*, 230–243. [[CrossRef](#)]
42. Morthorst, P.E. *Wind Energy—The Facts: Costs & Prices*; RISO National Laboratory: Roskilde, Denmark, 2010; Volume 2, pp. 94–110.
43. Dawn, S.; Tiwari, P.K. Improvement of economic profit by optimal allocation of TCSC & UPFC with wind power generators in double auction competitive power market. *Int. J. Electr. Power Energy Syst.* **2016**, *80*, 190–201. [[CrossRef](#)]
44. Basu, J.B.; Dawn, S.; Saha, P.K.; Chakraborty, M.R.; Ustun, T.S. Economic Enhancement of Wind–Thermal–Hydro System Considering Imbalance Cost in Deregulated Power Market. *Sustainability* **2022**, *14*, 15604. [[CrossRef](#)]
45. Tiwari, P.K.; Sood, Y.R. An Efficient Approach for Optimal Allocation and Parameters Determination of TCSC With Investment Cost Recovery Under Competitive Power Market. *IEEE Trans. Power Syst.* **2013**, *28*, 2475–2484. [[CrossRef](#)]
46. Das, A.; Dawn, S.; Gope, S.; Ustun, T.S. A Risk Curtailment Strategy for Solar PV-Battery Integrated Competitive Power System. *Electronics* **2022**, *11*, 1251. [[CrossRef](#)]